MULTI-SCALE LANDMARK SELECTION FOR IMPROVED REGISTRATION OF TEMPORAL MAMMOGRAMS

Marias K[1,2], Behrenbruch C.P.[1], Brady M[1], Parbhoo S[2], Seifalian A[2]

[1]Medical Vision Lab, Oxford University, United Kingdom

[2]Department of Surgery, Royal Free and University College Medical School, UCL, London, United Kingdom

1. Introduction

Mammogram registration remains a difficult problem, not least because of the many different and unpredictable changes observed in mammograms. For example, differences in imaging conditions for a pair of temporal mammograms induce a non-rigid transformation between their intensity profiles. Equally, even slight changes in breast compression lead to significant changes of the projected mammographic structures (Highnam and Brady 1999).

In this paper, we emphasise the need to establish correspondences between regions in temporal mammograms for robust and more accurate registration. Based on automatically detected boundary landmarks, we partially register, then subsequently analyse the mammogram pair using a non-linear wavelet scale-space to isolate significant regions of interest. We show that a usually small, but significant number of internal correspondences greatly improves registration and better approximates the complex internal tissue deformation due mainly to differences in compression.

2. Partial Registration using the boundary

Extensive experimentation has convinced us that registration based only on the breast edge does not accurately model the relative motions of important tissue regions under different levels of compression. Previous work with registration in mammogram registration has focused predominantly on aligning the boundary of the breast in each mammogram (Marias et al. 1999, Karssemeijer and Brake 1998). In our method, we automatically calculate the location of the nipple and the points between the breast, the rib cage and the axilla on the basis of separating positive and negative curvature portions of the breast edge and locating curvature peaks as shown in figure 1.

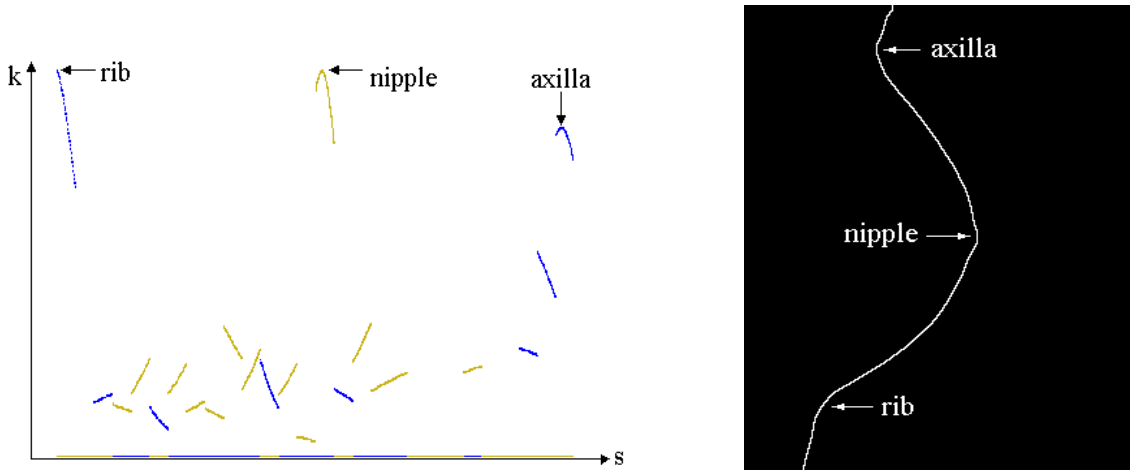

Figure 1: The curvature profile along the breast boundary k (*s*), consisting of the 2 peaks near both ends of the boundary (darker colour) and the peak corresponding to the nipple in the middle.

Next, we sample the breast edge between these points and partially register the images using thin-plate spline interpolation (Bookstein 1989). If the nipple is not visible in the breast outline, we sample between the axilla and the rib points. The boundary transformation accounts for the global differences between the images, correcting scaling (due to differences in compression or breast-size) translation and rotation due to breast positioning and orientation of the glandular

structures (since the nipple is included as a landmark). However, as described in (Kok-Wiles, Brady and Highnam 1998), different breast compressions (which are almost inevitable), tend to make denser structures (e.g. tumours) move much more than less denser tissues (like cysts or fibroglandular structures) resulting in an internal non-smooth motion field. Indeed, such differential motions are the basis for Highnam and Brady's differential compression technique, which aims to estimate tissue elasticity (Highnam and Brady 1999). The feature detection described in the next section aims at an intensity-invariant segmentation of "important" regions that can be matched as to better approximate internal tissue deformations.

3. Wavelet-based feature detection for refining registration

To complete the registration internal landmarks are required to compensate for the complexity of the soft-tissue deformations. To achieve this, a scale-space approach was chosen based on wavelet packets (Coifman et al 1992). Wavelet *packet* decompositions are linear superpositions of wavelets that result in large range of subspaces that have specific frequency and spatial localisations (Daubechies 1988). The scale space construction follows a conventional dyadic decomposition using filter bank of quadrature filters (QFs).

$$\psi_0 \triangleq L_f \psi_0; \qquad \int_R \psi_0(p).dp = 1,$$
$$\psi_{2n} \triangleq L_f \psi_n; \qquad \psi_{2n}(p) = \sqrt{2}\sum_{j\in Z} l_f(j)\,\psi_n(2p-j),$$
$$\psi_{2n+1} \triangleq H_f \psi_n; \qquad \psi_{2n+1}(p) = \sqrt{2}\sum_{j\in Z} h_f(j)\,\psi_n(2p-j),$$

Where: ψ_0 is the mother wavelet (filter) and ψ_{2n} and ψ_{2n+1} are the resulting wavelet subspaces after convolution and decimation with the low-pass/high-pass equivalent QFs h_f, l_f for pixel p (in one pixel vector). To date, we have used the Coiflet wavelet base as it yields good spatial

localisation (e.g. it is edge preserving), has compact support and is morphologically relevant, since is effective at detecting small regions such as microcalicifications.

After wavelet decomposition the scale-space is completed by using an information cost function in the context of a “best basis” algorithm (Coifman and Wickerhauser 1992) to order wavelet coefficients in such a way that the various subspaces used for the decomposition are ranked by information content. For this we use an entropy measure. Each wavelet subspace (filter superposition) is then cumulatively adjointly convolved, in order, with respect to the best-basis assessment of the decomposition. The result is a “stack” of reconstructions from minimum to maximum information content (dependent on the cost function). This construction is used to track significant features through scale space and forms the basis of our feature segmentation.

Based on the regions that are detected in this way, a set of internal landmarks is defined by a matching algorithm that includes the partial transformation (induced by the boundary alignment) in conjunction with scale, size and orientation information of the candidate matches. In most cases, as shown in figure 2, the segmented salient regions in the partially unwarped and the target image move towards each-other and exhibit a significant degree of overlap. Since only “important” bright regions that propagate in scale-space are isolated, the search space is small and the existence or not of a match for each region obvious. On average, depending on the degree to which the breast is involuted we define 3-5 internal landmarks at the centers of mass of the corresponding wavelet-defined regions.

The boundary points and the internal landmarks computed by the wavelet analysis together control a thin-plate spline approximation technique, which gives the final registration. The

matching algorithm provides a set of weights (the inverse of the variance σ_i^2) in order to characterise the uncertainty in the localisation of the landmarks.


(a)
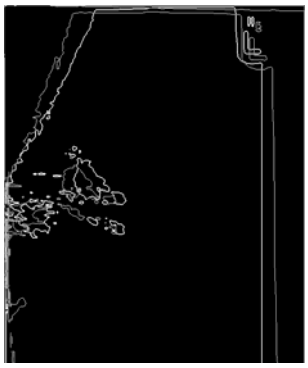
(b)

Figure 2: (a) Segmented "significant" regions between a temporal pair. (b) Superimposed regions between the "target" and the partially registered image. The corresponding regions "move" towards each other as the partial transformation approximates the motion under different compression.

The thin-plate spline approximation (Rohr et al. 1996), minimises the following functional:

$$J_\lambda(\mathbf{t}) = \sum_{i=1}^{n} \frac{\left|\mathbf{q}_i - \mathbf{t}(\mathbf{p}_i)\right|^2}{\sigma_i^2} + \lambda \cdot J_2^2(\mathbf{t})$$

Where $\mathbf{q}_i$ and $\mathbf{p}_i$ are the landmark pairs, $J_2(\mathbf{t})$ is the bending energy of the transformation $\mathbf{t}$ and λ is a regularisation parameter that controls the trade-off between the smoothness of the transformation and adaptation to the local transformations induced by the data. The global transformation smoothly transforms the boundary while local deformations occur on the inside according to the importance of the internal matches. The number of internal landmarks detected depends on the number of significant regions that propagate in the scale-space stack and are consistent in both images in the pair.

4. Results

In figure 3 (a) and (b), a temporal pair of mammogram is registered, first using just boundary points (figure 3(c) is the transformed 3(a)). Images 3 (d) and (e) show the matched regions based on the multi-scale wavelet analysis, superimposed onto images (c) and (b). Using the centers of mass of the corresponing regions, we re-register the images as described in section 3. The last image, 3 (f), is the resulting unwarped image. Figure 4 shows the difference image after the final registration (figure 4 (c)); it clearly shows the improvement in the registration (compared both to no registration and to the partial registration difference images in figures 4 (a) and (b)). Note that all the important features overlap, and the "shadows" corresponding to misregistations in figures 4(a) and (b) disappear. The deformation grid, shown in figure 5, is an alternative way to visualise the partial registration (figure 5 (b)) and the improved registration (figure 5 (c)).

This method has the potential also to be used to match bilateral mammograms pairs providing that a "structural" similarity exists. However, we have found that in many cases the architectural similarity between the breasts is not strong, and internal correspondences are difficult to establish. In figure 6, we see a bilateral pair where there is an obvious correspondence between the segmented (based on the wavelet analysis) regions.

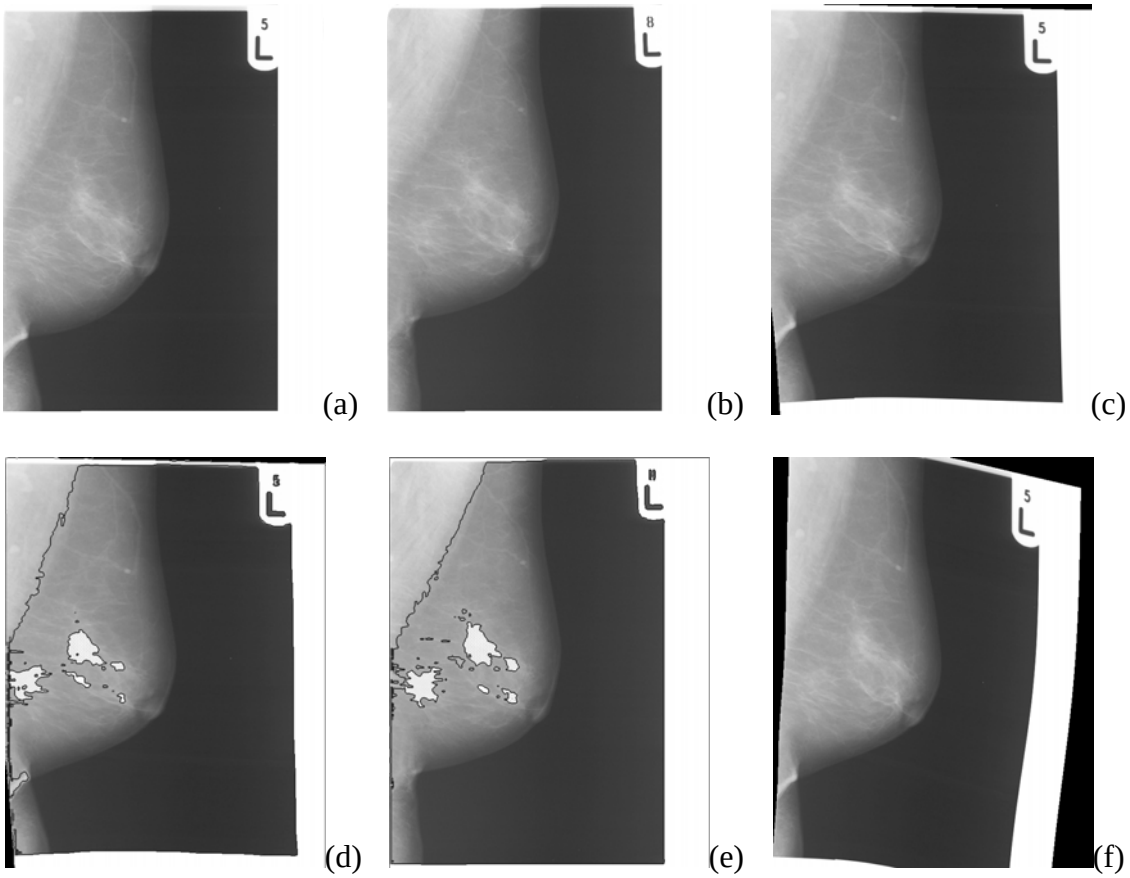

Figure 3 : (a) and (b): A temporal set of images, (c) Image (a) unwapred in the co-ordinates of image (b) using the boundary landmarks. (d) and (e): The matched regions based on the multi-scale wavelet analysis, superimposed to images (c) and (b), (f): The unwarped (a) to (b) after the final registration.

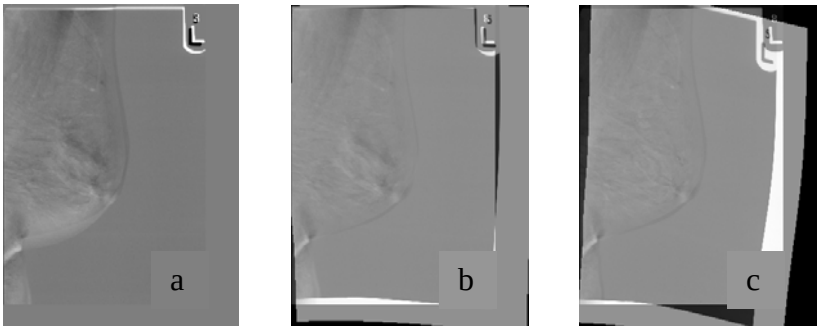

Figure 4: Difference images: (a): Before registration, (b): After partial registration and (c): After final registration including internal landmarks.

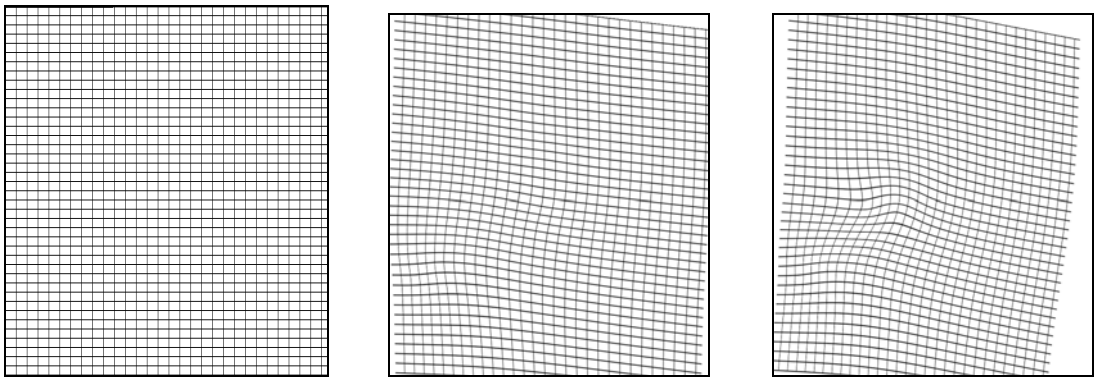

Figure 5: (a): The orthogonal grid, (b): The deformed grid for the partial transformation is relatively smooth inside the breast, (c): After the final registration the deformed grid depicts the relative non-smooth motion inside the breast under changing compression more realistically.

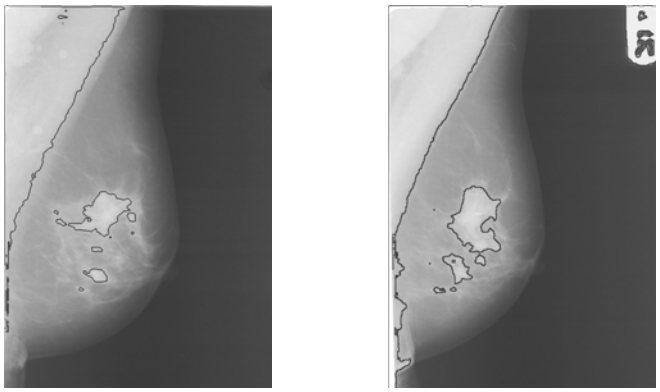

Figure 6: (a), (b): A bilateral pair of mammograms with the segmented "significant" regions superimposed. This clear correspondance of significant features is not always the case in bilateral mammograms.

5. Discussion

We have developed a method that improves registration of temporal mammograms. Multi-scale analysis provides a reliable framework for establishing correspondences between significant regions inside the breast. In this way, the algorithm presented here is an improvement on that presented by (Kok-Wiles, Brady and Highnam 1998). In a clinical assessment of the technique, an experienced radiologist judged that the correspondence between the registered images was improved in 20 out of 25 pairs of temporal mammograms, that were selected by the clinician.

The success of this method is limited by the degree of involution in the breast tissue. The more involuted the breast, the less “significant” internal structures we can detect using our method. Moreover, the 2-stage nature of the process ensures that at least the breast boundary can be aligned.

Mammogram registration could be a useful tool for aiding the clinician to detect abnormalities by comparing a mammogram with a previous one, as significantly “different” regions are easily detected in the difference image (after registration) (Marias et al. 1999). In addition, we recently used the same registration technique to align HRT sequences in order to assess overall changes in tissue composition and to be able to estimate the site of local changes in tissue density: a report of that work is currently in preparation. Finally, C.P Behrenbruch has used the same technique (which he co-developed) for 3D-MRI to 2D-xray data fusion (Behrenbruch et al. 2000). All these possible aplications of temporal mammogram registration encourage us to believe that even though it is a difficult engineering problem, fully- or semi-automatic mammogram registration has an important role to play in the future of digital mammography.

REFERENCES

Behrenbruch C.P., K. Marias, P.A. Armitage, M. Yam, N. Moore, R. E. English, J. M. Brady. 2000. MRI - Mammography 2D/3D Data Fusion for Breast Pathology Assessment. Submited to *MICCAI 2000*.

Bookstein F.1989. Principal warps: Thin-plate splines and the decomposition of deformations.

Coifman R.R., M.V.Wickerhauser. 1992. Entropy based algorithms for best basis selection, *IEEE Transactions on Information Theory*, 32: 712-71.

Coifman, R.R., Y.Meyer, S.R. Quake, M.V. Wickerhauser. 1992. Signal processing and compression with wavelet packets. In *Meyer and Roques*, pp 77-93.

Daubechies, I. 1988. Orthonormal bases of compactly supported wavelets. *Communications on Pure and Applied Mathematics,* XLI:909-996.

Highnam R.P., and J.M. Brady. 1999. *Mammographic image processing*. Kluwer Academic Press.

Karssemeijer N. and G.T. Brake. 1998. Combining single view features and asymmetry for detection of mass lesions. In Proceedings of *Digital Mammography 98*, pp. 95-102, Kluwer Academic Publisher, Nijmegen.

Kok-Wiles Siew-Li, M. Brady and R.Hignam. 1998. Comparing mammogram pairs for the detection of lesions. In Proceedings of *Digital Mammography 98*, pp. 103-110, Kluwer Academic Publisher, Nijmegen 1998.

Marias K., J.M. Brady, R.P. Highnam, S. Parbhoo, and A.M. Seifalian. 1999. Registration and matching of temporal mammograms for detecting abnormalities. In Proceedings of *Medical Imaging Understanding and Analysis*.

Rohr K., H.S. Stiehl, R Sprengel, W.Beil, T.M. Buzug, J.Weese, and M.H. Kuhn. 1996. Point-based elastic registration of medical image data using approximating thin-plate splines. *Lecture notes in computer Science* 1131: 297-306.